



# A fluorimetric study of the interaction of C.I. Solvent Red 24 with haemoglobin

Hong-Mei Zhang<sup>a,b</sup>, Yan-Qing Wang<sup>a,b,\*</sup>, Ma-Li Jiang<sup>a,b</sup>

<sup>a</sup> Jiangsu Provincial Key Laboratory of Coastal Wetland Bioresources and Environmental Protection, Yancheng City, Jiangsu Province 224002, People's Republic of China

<sup>b</sup> Institute of Applied Chemistry and Environmental Engineering, Yancheng Teachers University, Yancheng City, Jiangsu Province 224002, People's Republic of China

## ARTICLE INFO

### Article history:

Received 1 October 2008

Received in revised form

18 December 2008

Accepted 20 December 2008

Available online 3 January 2009

### Keywords:

Haemoglobin

C.I. Solvent Red 24

Fluorescence spectroscopy

Binding constant

Thermodynamic parameters

Three-dimensional fluorescence spectra

## ABSTRACT

The interaction between bovine haemoglobin and C.I. Solvent Red 24 was investigated by UV/vis absorption, fluorescence, resonance light-scattering spectra, synchronous fluorescence as well as three-dimensional fluorescence spectra techniques at pH 7.4. The dye effectively quenched the intrinsic fluorescence of bovine haemoglobin via static quenching. The process of dye to bovine haemoglobin was spontaneous, the related changes in enthalpy and entropy being  $1.78 \text{ kJ mol}^{-1}$ ,  $81.58 \text{ J mol}^{-1} \text{ K}^{-1}$  respectively, according to the van't Hoff equation, indicating that hydrophobic interaction played a major role in stabilizing the complex. Synchronous fluorescence spectroscopy and three-dimensional fluorescence spectra showed that the structure of the tyrosine residue environments was altered by the dye which interacted at the  $\alpha_1\beta_2$  interface of the bovine haemoglobin molecule.

© 2008 Elsevier Ltd. All rights reserved.

## 1. Introduction

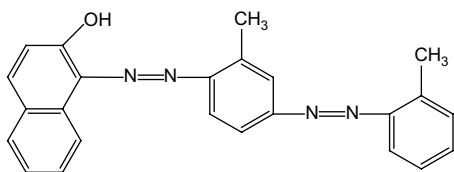
C.I. Solvent Red 24 (Sudan IV,  $\text{C}_{24}\text{H}_{20}\text{N}_4\text{O}$ , Scheme 1) is a lysochrome (fat-soluble dye) diazo dye used to color nonpolar substances like oils, fats, waxes, greases, various hydrocarbon products, and acrylic emulsions in industry [1,2]. However, as a food dye, C.I. Solvent Red 24 (SR24) is considered an illegal dye, mainly because of its harmful effect over a long period of time, as it is a carcinogen. It was ruled unsafe in the 1995 food safety regulations report. Sudan I, Sudan III, and Sudan IV have been classified as category 3 carcinogens by the International Agency for Research on Cancer [3]. Although recognized as carcinogens, Sudan dyes have been found recently in food products in some European countries. They are added to food such as chilli powder to mimic, intensify, and prolong the appearance of natural red hues. In UK, more than six hundred products containing Sudan dyes have been recalled such as fish sauce, Worcestershire sauce, noodle soup, and pizza [2,4]. In China and some other Asian countries, it is said that the redder the egg yolk is, the more nutrient it is. So Sudan dyes are illegally added into feedstuffs and feed poultry, such as ducks and hens. Consequently, the dyes are enriched in egg yolk, and the red-yolk

eggs are produced [5]. From the toxicological viewpoint, several studies have been carried out in order to check the noxious effects on humans [6].

Since the overall distribution, metabolism and efficacy of many drugs are correlated with their affinities towards haemoglobin (Hb) [7,8], the investigation of drugs with respect to Hb-drug binding is imperative and of fundamental importance. Hb is one of some ordinary proteins, consisting of two identical  $\alpha$ -chains of 141 amino acids each and two identical  $\beta$ -chains of 146 amino acids each [9]. Hb is well known for its function in the vascular system of animals, being a carrier of oxygen. It also aids, both directly and indirectly, the transport of carbon dioxide and regulates the pH of blood [10]. In addition, it is involved in many clinical diseases such as leukemia, anemia, heart disease, excessive loss of blood, etc. [11]. Several reports were published on the interactions of hematoporphyrin [12], Pt drugs [7], artemisinins [8], surfactant [13], aromatic amines [14], flavonoids [15,16] and herbicide [17] with haemoglobin. Studying structural dynamics of dye-protein complexes is crucial for understanding the biological effects and functions of dyes in body. Interaction between dye and protein governs the duration and intensity of pharmacological effect [18]. Seetharamappa et al. have studied the binding of bromopyrogallol red and rose bengal to bovine serum albumin in order to investigate that the dyes exhibit a high affinity to bovine serum albumin [19,20]. Yue et al. have studied the binding of C.I. Direct Yellow 9 to human serum albumin using optical spectroscopy and molecular modeling [18]. Zhang and coworkers have studied the binding of Sudan I to bovine serum

\* Corresponding author. Institute of Applied Chemistry and Environmental Engineering, Yancheng Teachers University, Yancheng City, Jiangsu Province 224002, People's Republic of China. Tel.: +86 515 88265276; fax: +86 515 88233188.

E-mail address: [wyqing76@126.com](mailto:wyqing76@126.com) (Y.-Q. Wang).



**Scheme 1.** The molecule structure of C.I. Solvent Red 24.

albumin [21]. However, to the best of our knowledge, the detailed investigation of SR24–Bhb association using fluorescence spectroscopy is not reported in the literature. The mode of interaction, association constant and number of binding sites are important; these investigations may provide some important theoretic information for the improvement of the metabolism and distribution of SR24 in life science. In this report, we provide investigations on the effect of SR24 on the structural and optical properties of Bhb, the thermodynamic aspects in the binding process, and characters of the binding sites by UV/vis absorption, fluorescence, resonance light-scattering spectra (RLS), synchronous fluorescence, and three-dimensional fluorescence spectra techniques under physiological pH 7.40. The results may cast some light on the future study of the interaction between Sudan dyes and other proteins such as enzymes and have toxicological importance; our work should be valuable in ecotoxicology.

## 2. Materials and methods

### 2.1. Materials

Bhb and SR24 were purchased from Sigma (St. Louis, MO, USA). The buffer tris was purchased from Acros (Geel, Belgium), and NaCl, HCl, etc. were all of analytical purity. Bhb solution (3.0  $\mu\text{M}$ ) was prepared in pH 7.40 Tris–HCl buffer solution (0.05 M Tris, 0.1 M NaCl). The SR24 solution (1.25 mM) was prepared in ethanol containing 10% DMSO (v/v) because of its low solubility.

### 2.2. Equipment and spectral measurements

The UV/vis spectra were recorded at room temperature on an SPECORD S 600 (Germany) equipped with 1.0 cm quartz cells. All fluorescence spectra were recorded on LS–50B Spectrofluorimeter (Perkin–Elmer USA) equipped with 1.0 cm quartz cells and a thermostat bath. The widths of both the excitation slit and the emission slit were set to 10.0 nm/5.0 nm for Bhb, respectively.

### 2.3. Procedures

A 2.5 mL solution, containing appropriate concentration of Bhb, was titrated by successive additions of a 1.25 mM stock solution of SR24 (to give a final concentration of 42.0  $\mu\text{M}$ ). Titrations were done manually by using trace syringes. The fluorescence spectra were then measured (excitation at 280 nm and emission wavelengths of 290–400 nm) at two temperatures (298 K, 308 K). Wherever applicable, the tryptophan fluorescence from Bhb has been corrected for inner filter effect due to the absorbance by SR24 at the excitation ( $\lambda_{\text{ex}}$  = 280 nm) and emission wavelength ( $\lambda_{\text{em}}$  = 336 nm) according to the procedure given in Ref. [22]. The three-dimensional fluorescence spectrum was performed under the following conditions: the emission wavelengths at 200–500 nm, the excitation at 220 nm, scanning number 15 and increment 10 nm with other parameters just the same as those of the fluorescence quenching spectra. The UV/vis absorbance spectra of SR24 and Bhb were recorded at room temperature. Resonance

light-scattering spectra (RLS) spectra were obtained by synchronous scanning with the wavelength range of 200–700 nm on the spectrofluorophotometer at room temperature.

## 3. Results and discussion

### 3.1. Interaction between SR24 and Bhb

UV/vis absorption spectroscopy is a very simple method and applicable to explore the structural change and to explore complex formation [23]. As shown in Fig. 1(A), SR24 gives two characteristic absorption bands at 220 nm ( $n \rightarrow \sigma^*$ ) and 520 nm ( $\pi \rightarrow \pi^*$ ). Upon complexation with Bhb, the 220 nm band of SR24 experiences red shift and the 520 nm band experience an obvious blue shift. Fig. 1(B) shows that the absorption wavelengths of Bhb and the difference absorption spectrum between Bhb–SR24 and SR24. The absorption band of 222 nm of Bhb is the characteristic of  $\alpha$ -helix structure of Bhb. The UV/vis absorption spectrum of Bhb also shows a band in the near-UV region with a maximum at 275 nm, which appears due to phenyl group of tryptophan residues (Trp) and tyrosines. The peak at 410 nm corresponds to the Soret-band of Bhb. Clearly, the absorbance (222 nm) of Bhb–SR24 system has decreased and the peak has a red shift (from 222 nm to 230 nm). The results from Fig. 1(A) and (B) indicated that there exists interaction between SR24 and Bhb and ground state complex has formed.

For macromolecules, the fluorescence measurements can give some information of the binding of small molecule substances to

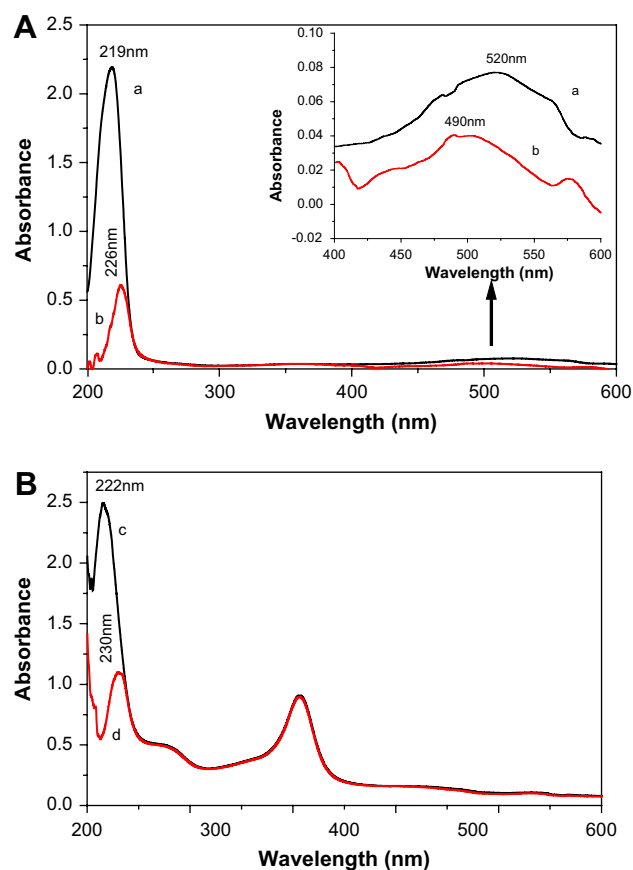


**Fig. 1.** Absorption spectra of SR24, Bhb, and Bhb–SR24 system. a, the absorption spectrum of SR24 only; b, the difference absorption spectrum between Bhb–SR24 and SR24; c, the absorption spectrum of Bhb only; d, the difference absorption spectrum between Bhb–SR24 and SR24, c (Bhb) = 3.0  $\mu\text{M}$ , c (SR24) = 3.0  $\mu\text{M}$ .

protein on the molecular level, such as the binding mechanism, binding mode, binding constants, binding studies, intermolecular distances, etc. BHb contains three Trp residues in each  $\alpha\beta$  dimer, for a total of six in the tetramer: two  $\alpha$ -14 Trp, two  $\beta$ -15 Trp, and  $\beta$ -37 Trp. The intrinsic fluorescence of BHb primarily originates from  $\beta$ -37 Trp that plays a key role in the quaternary state change upon ligand binding [24]. A valuable feature of intrinsic fluorescence of a protein is the high sensitivity of tryptophan to its local environment. Changes in emission spectra of tryptophan are common in response to protein conformational transitions, subunit association, substrate binding, or denaturation [25]. Thus, the intrinsic fluorescence of proteins can provide considerable information about their structure and dynamics, and is often considered on the study of protein folding and association reactions.

Generally speaking, the fluorescence quenching is the decrease of the quantum yield of fluorescence from a fluorophore induced by a variety of molecular interactions with quencher molecule, such as excited-state reaction, molecules rearrangement, energy transfer, ground state complex formation and collision quenching. The effect of SR24 on BHb fluorescence intensity is shown in Fig. 2. As the data show, the fluorescence intensity of BHb decreased regularly with the increasing concentration of SR24. In order to confirm the quenching mechanism, the fluorescence quenching data are analyzed by the Stern–Volmer equation [26]:

$$\frac{F_0}{F} = 1 + k_q \tau_0 [Q] = 1 + K_{SV} [Q] \quad (1)$$

where  $F_0$  and  $F$  are the fluorescence intensities before and after the addition of the quencher, respectively.  $k_q$ ,  $K_{SV}$ ,  $[Q]$ , and  $\tau_0$  are the quenching rate constant of the bimolecular, the Stern–Volmer dynamic quenching constant, the concentration of the quencher and the average lifetime of the Hb without quencher, respectively. Some previous studies have determined that the lifetime of tryptophan in the haemoglobin system is 5.0 ns [27]. As a rule, the maximum scatter collision quenching constant,  $K_q$  of various quenching with the biopolymer was  $2.0 \times 10^{10} \text{ L mol}^{-1} \text{ s}^{-1}$  [28]. Fig. 3 displays the Stern–Volmer plots of the quenching of BHb tryptophan residues' fluorescence by SR24 at different temperatures. The plot showed that within the investigated concentrations, the results agreed with the Stern–Volmer Eq. (1). The Stern–Volmer did not show deviation towards the y-axis obviously at the experimental concentration range, which was an indication that either dynamic quenching or static quenching was predominant [17]. In Table 1, the binding constants obtained from the Stern–Volmer

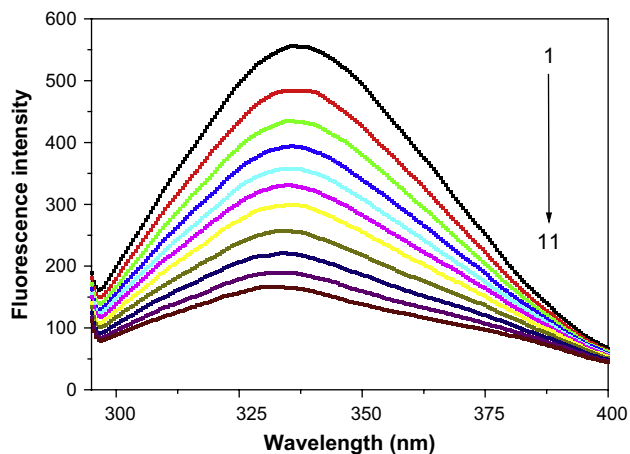


Fig. 2. Effect of SR24 on fluorescence spectra of BHb ( $T = 298 \text{ K}$ ,  $\text{pH} = 7.40$  and  $\lambda_{\text{ex}} = 280 \text{ nm}$ ).  $c(\text{BHb}) = 3.0 \mu\text{M}$ ,  $c(\text{SR24})/(\mu\text{M})$ , curve (1–11): 0, 3.0, 6.0, 9.0, 12.0, 15.0, 18.0, 24.0, 30.0, 36.0, and 42.0, respectively.

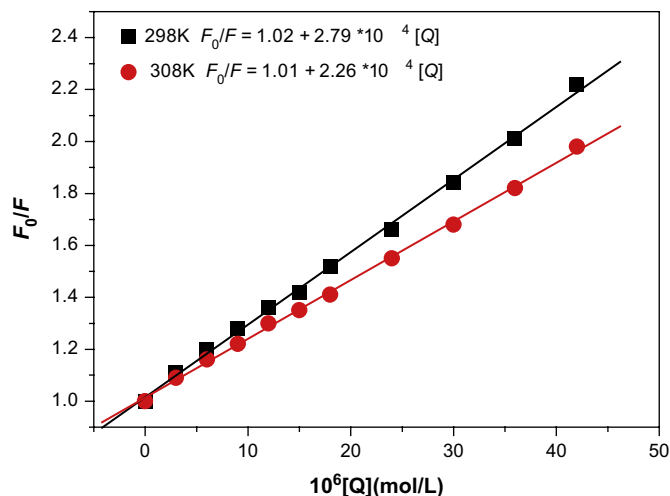


Fig. 3. Stern–Volmer plots for the quenching of BHb by SR24 at different temperatures. BHb concentration was at  $3.0 \mu\text{M}$ ,  $\text{pH} = 7.40$ ,  $\lambda_{\text{ex}} = 280 \text{ nm}$  and  $\lambda_{\text{em}} = 336 \text{ nm}$ .

method are listed for SR24 with BHb. The  $K_q$  was the order of  $10^{12} \text{ L mol}^{-1} \text{ s}^{-1}$ . Obviously, the  $K_q$  value of protein quenching procedure initiated by SR24 was greater than  $2.0 \times 10^{10} \text{ L mol}^{-1} \text{ s}^{-1}$ . This indicated that the quenching was not initiated from dynamic collision but from the formation of a complex. Furthermore, the blue shift of the emission maximum observed in the BHb–SR24 system indicated the occurrence of conformational changes for BHb at tertiary structure levels since the shift in the position of emission maximum reflected the changes of the polarity around the Trp residues [29].

Red edge excitation shift (REES) is a shift in the emission maximum toward a higher wavelength caused by a shift in the excitation wavelength toward the red edge of the absorption band [29]. The REES is due to the electronic coupling between Trp indole rings and neighboring dipoles and occurs when there are slow relaxations of solvent media. Thus, REES is particularly useful in monitoring motions around the Trp residues in protein studies [30]. The Trp emission in the BHb–SR24 system was further investigated by red edge excitation shift (REES) experiments [31]. In our experiment, we chose to excite the Trp at both 295 and 305 nm to investigate the REES effect, and the results are listed in Table 2. The value of  $\Delta\lambda_{\text{em max}}$  is defined as the difference of the emission maximum between that excited at 295 nm and at 305 nm. As shown, native BHb showed a 1.0 nm REES, indicating that Trp residues in the haemoglobin were in a slight motionally restricted environment. In the presence of SR24, the values all showed an increase. The increase of  $\Delta\lambda_{\text{em max}}$  meant that the introduction of SR24 had an obvious impact on the mobility of the Trp microenvironment and that Trp residues faced more restrictions from their surroundings in the BHb–SR24 system [29].

### 3.2. Binding constant and binding capacity

SR24-induced fluorescence quenching data of BHb were analyzed to obtain various binding parameters. The binding

Table 1  
Stern–Volmer quenching constants of the system of BHb–SR24.

pH	$T$ (K)	$10^{-4} \cdot K_{SV} (\text{L mol}^{-1})$	$10^{-12} K_q (\text{L mol}^{-1})$	$R^a$	$SD^b$
7.40	298	2.79	5.58	0.9976	0.0612
	308	2.26	4.52	0.9983	0.0513

<sup>a</sup> The correlation coefficient.

<sup>b</sup> The standard deviation.

**Table 2**  
Red edge excitation effects for BHb and BHb–SR24 system.

Sample		$\lambda_{\text{em max}}$ (nm)		$\Delta\lambda_{\text{em max}}$ (nm)
		$\lambda_{\text{ex}}: 295 \text{ nm}$	$\lambda_{\text{ex}}: 305 \text{ nm}$	
BHb		337	338	1
BHb–SR24	1:5	336	338	2
[n(BHb):n(SR24)]	1:10	331.5	336.5	5

constant ( $K_A$ ) and binding affinity ( $n$ ) were calculated using equation [14,32]

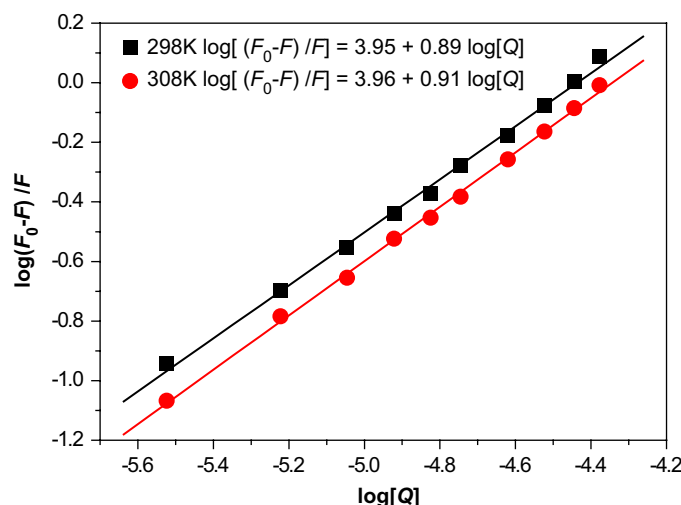
$$\log \left[ \frac{F_0 - F}{F} \right] = \log K_A + n \log [Q] \quad (2)$$

Fig. 4 shows the plots of  $\log (F_0 - F)/F$  vs.  $\log [Q]$  for the BHb–SR24 system at different temperatures obtained from the fluorometric titration. In Table 3, the binding constants  $K_A$  and binding sites  $n$  were listed for SR24 associated with BHb. The results showed that the binding constants  $K_A$  were increased with the temperature, which indicated that the binding is an endothermic reaction [33,34]. The BHb–SR24 complex is easily formed with the rising temperature. The values of  $n$  at the experimental temperatures were approximately equal to 1, which indicated that there was one class of binding sites to SR24 in BHb. The intrinsic fluorescence of BHb primarily originates from  $\beta$ -37 Trp, which indicated that SR24 binding site on BHb was located closer to the  $\beta$ -37 Trp.

### 3.3. Thermodynamic parameters and nature of the binding forces

There are essentially four types of noncovalent interactions that could play a role in ligand binding to proteins. These are hydrogen bonds, van der Waals forces, electrostatic, and hydrophobic interactions [35]. To obtain such information, the implications of the present results have been discussed in conjunction with thermodynamic characteristics obtained for SR24 binding, and the thermodynamic parameters were calculated from the Van't Hoff equation.

$$\ln \frac{(K_A)_2}{(K_A)_1} = \frac{\Delta H^\circ}{R} \left( \frac{1}{T_1} - \frac{1}{T_2} \right) \quad (3)$$



**Fig. 4.** The plots of  $\log [(F_0 - F)/F]$  vs.  $\log [Q]$  at different temperatures for BHb.  $c$  (BHb) = 3.0  $\mu\text{M}$ ; pH = 7.40;  $\lambda_{\text{ex}}$  = 280 nm,  $\lambda_{\text{em}}$  = 336 nm.

$$\Delta G^\circ = -RT \ln K_A \quad (4)$$

$$\Delta S^\circ = \frac{\Delta H^\circ - \Delta G^\circ}{T} \quad (5)$$

From Table 3, it can be seen that the negative sign for  $\Delta G^\circ$  indicated the spontaneity of the binding of SR24 with BHb. The enthalpy change ( $\Delta H^\circ$ ) and entropy change ( $\Delta S^\circ$ ) were positive values. The main source of  $\Delta G^\circ$  value was derived from a large contribution of  $\Delta S^\circ$  term with little contribution from the  $\Delta H^\circ$  factor. Ross and Subramanian [35] have characterized the sign and magnitude of the thermodynamic parameter associated with various individual kinds of interaction that may take place in protein association processes. From the point of view of water structure, a positive  $\Delta S^\circ$  value is frequently taken as evidence for hydrophobic interaction. The interaction of SR24 with BHb included the hydrophobic forces between the aromatic ring and the hydrophobic amino acid residues. Accordingly, it was more likely that hydrophobic interaction was involved in its binding process. SR24 could enter into the hydrophobic pocket of BHb.

### 3.4. Characteristics of the RLS spectra

The RLS spectra of BHb, BHb–SR24 complex are recorded by synchronous scanning from 200 to 700 nm with  $\Delta\lambda = 0$  nm. The results are shown in Fig. 5. Upon addition of trace amount of Suda IV to BHb solution, a remarkably decreased RLS was observed (Fig. 5A and B). The production of RLS is correlated with the formation of certain aggregate and the RLS intensity is dominated primarily by the particle dimension of the formed aggregate in solution [36]. Bearing these points in mind, it is inferred from the results that the added SR24 may interact with BHb in solution, forming a new BHb–SR24 complex that could be expected to be an aggregate. The newly formed BHb–SR24 complex may be ascribed to the higher electrostatic attraction between SR24 and BHb. The size of BHb–SR24 particles may be smaller than that of BHb, and thus the decreased light-scattering signal occurred under the given conditions.

### 3.5. Energy transfer from BHb to SR24

Fluorescence resonance energy transfer (FRET) is a distance dependent interaction between the different electronic excited states of dye molecules in which excitation energy is transferred from one molecular system (donor) to another molecular system (acceptor) without emission of a photon from the former molecular system. FRET is an important technique for investigating the structure, conformation spatial distribution and assembly of complex proteins. According to Förster's theory [37], the efficiency of FRET depends mainly on the following factors: (i) the extent of overlap between the donor emission and the acceptor absorption, (ii) the orientation of the transition dipole of donor and acceptor, and (iii) the distance between the donor and the acceptor. Here the donor and acceptor were BHb and SR24, respectively. There was a spectral overlap between the fluorescence emission spectrum of free BHb and absorption UV/vis spectra of SR24 (Fig. 6). The spectrum ranging from 295 to 400 nm was chosen to calculate the overlapping integral.

According to Förster's theory the energy transfer efficiency  $E$  is defined as the following equation Eq. (6). Where  $r$  is the distance from the ligand to the tryptophan residue of the protein, and  $R_0$  is the Förster critical distance, at which 50% of the excitation energy is transferred to the acceptor [37]. It can be calculated from donor emission and acceptor absorption spectra using the Förster formula Eq. (7).



**Table 3**

Thermodynamic parameters of BHb–SR24 interaction at pH 7.40.

<i>T</i> (K)	$10^{-3} K_A$ (L mol <sup>-1</sup> )	<i>n</i>	<i>R</i> <sup>a</sup>	<i>SD</i> <sup>b</sup>	$\Delta H^\circ$ (KJ mol <sup>-1</sup> )	$\Delta G^\circ$ (KJ mol <sup>-1</sup> )	$\Delta S^\circ$ (J mol <sup>-1</sup> K <sup>-1</sup> )
298	8.91	0.89	0.9983	0.0198	1.78	–22.53	81.58
308	9.12	0.91	0.9992	0.0143		–23.35	

<sup>a</sup> The correlation coefficient.<sup>b</sup> The standard deviation.

$$E = 1 - \frac{F}{F_0} = \frac{R_0^6}{R_0^6 + r^6} \quad (6)$$

$$R_0^6 = 8.79 \times 10^{-25} K^2 N^{-4} \phi J \quad (7)$$

$$J = \frac{\int_0^\infty F(\lambda) \varepsilon(\lambda) \lambda^4 d\lambda}{\int_0^\infty F(\lambda) d\lambda} \quad (8)$$

In Eq. (7),  $K^2$  is the orientation factor related to the geometry of the donor and acceptor of dipoles and  $K^2 = 2/3$  for random orientation as in fluid solution;  $N$  is the average refractive index of medium in the wavelength range where spectral overlap is significant;  $\phi$  is the fluorescence quantum yield of the donor;  $J$  is the effect of the spectral overlap between the emission spectrum of the donor and the absorption spectrum of the acceptor (Fig. 6), which could be calculated by Eq. (8), where,  $F(\lambda)$  is the corrected fluorescence intensity of the donor in the wavelength range  $\lambda$  to  $\lambda + \Delta\lambda$ ;  $\varepsilon(\lambda)$  is the extinction coefficient of the acceptor at  $\lambda$ . In the present case,  $N = 1.36$ ,  $\phi = 0.06$  [38], according to Eqs. (6)–(8), we could calculate that  $J = 1.32 \times 10^{-14} \text{ cm}^3 \text{ L mol}^{-1}$ ,  $E = 0.13$ ,  $R_0 = 2.82 \text{ nm}$ ,  $r = 3.87 \text{ nm}$ . The average distance between a donor fluorophore and acceptor fluorophore was on the 2–8 nm scale, which indicated that the energy transfer from BHb to SR24 occurred with high probability [39], while  $r$  was bigger than  $R_0$  in the present study also revealed that SR24 could strongly quench the intrinsic fluorescence of BHb by static quenching.

### 3.6. Conformation investigation

To explore the structural change of BHb by addition of SR24, we measured synchronous fluorescence spectra of trypsin (Fig. 7) with various amounts of SR24.

Synchronous fluorescence spectroscopy technique was introduced by Lloyd [40] and involves simultaneous scanning of the

excitation and emission monochromators while maintaining a constant wavelength interval between them. The synchronous fluorescence spectroscopy gives information about the molecular environment in a vicinity of the chromosphere molecules and has several advantages, such as sensitivity, spectral simplification, spectral bandwidth reduction and avoiding different perturbing effects [23]. When the  $D$ -value ( $\Delta\lambda$ ) between excitation wavelength and emission wavelength were stabilized at 15 nm or 60 nm, the synchronous fluorescence gives the characteristic information of tyrosine residues or tryptophan residues [41]. The effect of SR24 on BHb synchronous fluorescence spectroscopy is shown in Fig. 7.

It was apparent from Fig. 7 that the emission maximum of tyrosine residues did significantly blue shift which indicated that the conformation of BHb was changed, the polarity around the tyrosine residues was decreased and the hydrophobic was increased. This may be due to the changes of residue microenvironment with the insertion of SR24. BHb contains three Trp residues in each  $\alpha\beta$  dimer, for a total of six in the tetramer: two  $\alpha$ -14 Trp, two  $\beta$ -15 Trp, and  $\beta$ -37 Trp, the  $\alpha$ -14 Trp and  $\beta$ -15 Trp residues are outside the subunit interface [42]. The  $\beta$ -37 Trp residue is located at the  $\alpha_1\beta_2$  interface, which has been assigned as the primary source of fluorescence emission. The aromatic residues of  $\alpha$ -42 Tyr,  $\alpha$ -140 Tyr, and  $\beta$ -145 Tyr are also located at the  $\alpha_1\beta_2$  interface [43]. The blue shift observed in Fig. 7(A) indicated that SR24 molecular is close enough to the phenyl moiety of Tyr residues during the binding process. It has been also shown in Fig. 8 that the slope was higher when  $\Delta\lambda$  was 60 nm indicating that a significant contribution of Trp residues in the fluorescence of BHb–SR24 could enter into the hydrophobic pocket at the  $\alpha_1\beta_2$  interface of BHb.

The three-dimensional fluorescence contour maps are a rising fluorescence analysis technique in recent years. The excitation wavelength, the emission wavelength and the fluorescence intensity can be used as the axes in order to investigate the synthetically information of the samples, and the contour spectra can also provide a lot of important information [44]. The three-dimensional fluorescence contour map of BHb (A) and BHb–SR24 (B, C) are

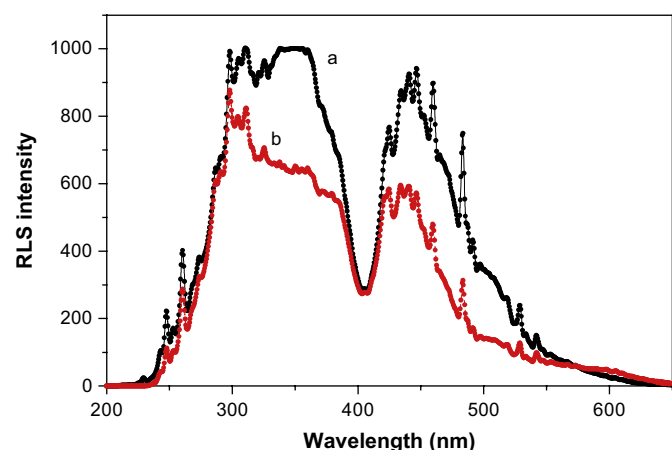


Fig. 5. RLS spectra of BHb(a), BHb–SR24 complex (b), c (BHb) = 3.0  $\mu\text{M}$  c (SR24) = 15.0  $\mu\text{M}$ .

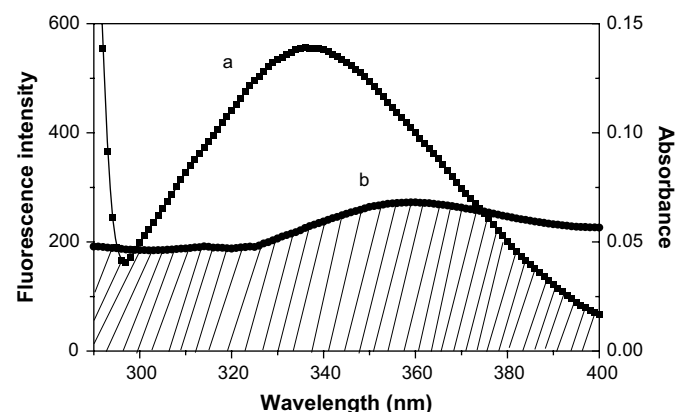
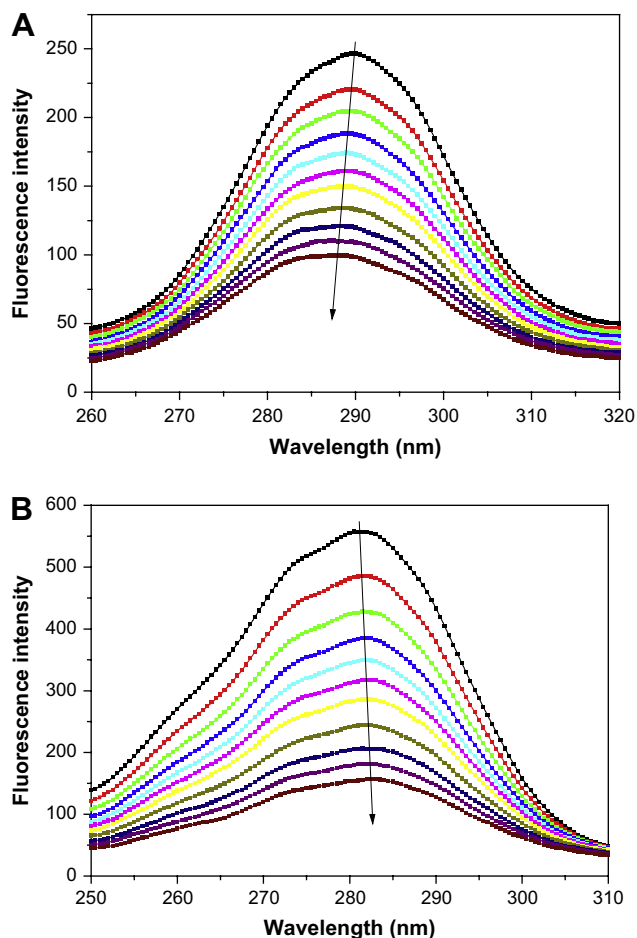
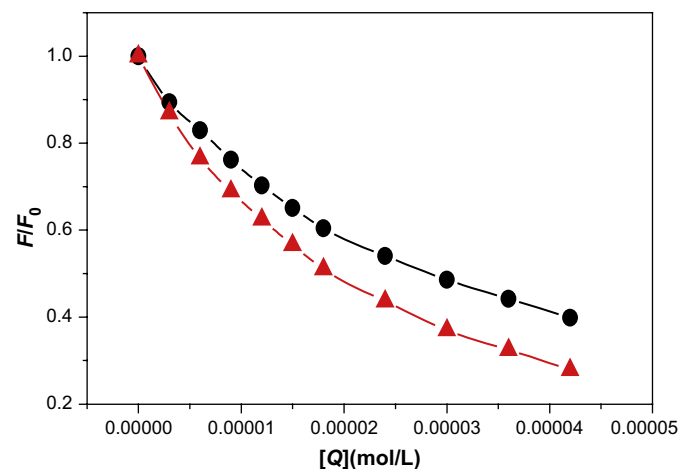


Fig. 6. Overlap of the fluorescence emission of BHb (a) with the absorption spectra of SR24 (b), c(BHb) = 3.0  $\mu\text{M}$ , c(SR24) = 6.0  $\mu\text{M}$ .



**Fig. 7.** Synchronous fluorescence spectrum of BHb ( $T = 298\text{K}$ ,  $\text{pH} = 7.40$ ),  $c(\text{BHb}) = 3.0\text{ }\mu\text{M}$ ;  $c(\text{SR24})/(\mu\text{M})$ , curve (from up to down): 0, 3.0, 6.0, 9.0, 12.0, 15.0, 18.0, 24.0, 30.0, 36.0, and 42.0, respectively. (A)  $\Delta\lambda = 15\text{ nm}$  and (B)  $\Delta\lambda = 60\text{ nm}$ .

presented Fig. 9. The contour map displayed a bird's eye view of the fluorescence spectra. The result showed that three-dimensional fluorescence contour map of BHb and BHb-SR24 was obviously different. In Fig. 9(A), two typical fluorescence peaks could be easily observed in three-dimensional fluorescence contour map of BHb. As referred to peak B, we think that it mainly reveals the spectral



**Fig. 8.** The quenching of BHb synchronous fluorescence by SR24. The concentration of BHb at  $3.0\text{ }\mu\text{M}$  (●)  $\Delta\lambda = 15\text{ nm}$  and (▲)  $\Delta\lambda = 60\text{ nm}$ .

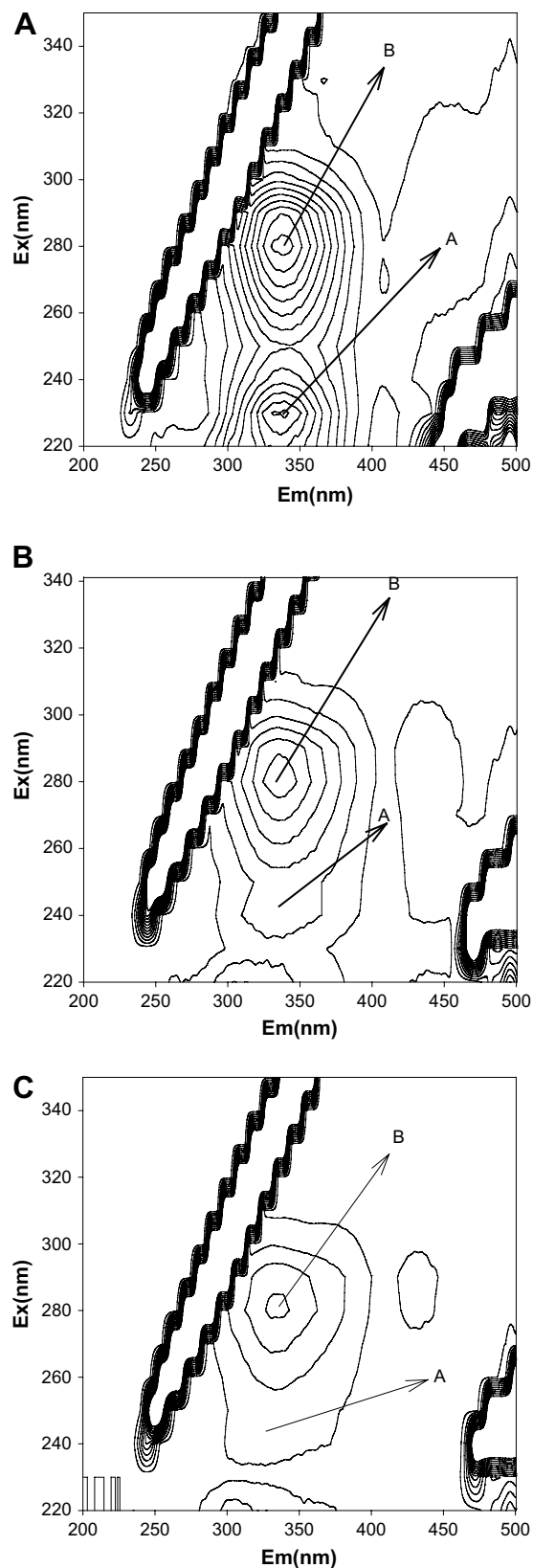


**Fig. 9.** The three-dimensional fluorescence contour map of BHb (A) and BHb-BHb (B, C) [the concentration of BHb: A  $3.0\text{ }\mu\text{M}$ , B  $3.0\text{ }\mu\text{M}$ , C  $3.0\text{ }\mu\text{M}$ ; the concentration of SR24: A  $0\text{ }\mu\text{M}$ , B  $15.0\text{ }\mu\text{M}$ , C  $30.0\text{ }\mu\text{M}$ ].

**Table 4**

Three-dimensional fluorescence spectral characteristics of BHb and Bhb-SR24 system.

System		Peak A ( $\lambda_{\text{ex}}/\lambda_{\text{em}}$ )	$\Delta\lambda$ (nm)	Intensity	Intensity ratio	Peak B ( $\lambda_{\text{ex}}/\lambda_{\text{em}}$ )	$\Delta\lambda$ (nm)	Intensity
BHb		230/339	109	517.07	0.90:1	280/339	59	576.28
BHb-SR24	1:5	240/336	96	132.89	0.40:1	280/336	56	334.43
[n(BHb):n(SR24)]	1:10	240/326	86	71	0.34:1	280/334	54	210.46

characteristics of tryptophan and tyrosine residues. The reason is that when serum albumin is excited at 280 nm, it mainly reveals the intrinsic fluorescence of tryptophan and tyrosine residues. Comparing with the UV/vis absorbance spectra of BHb (Fig. 1(B), curve c), there is an absorption peak around 275 nm and this peak is mainly caused by the transition of  $\pi \rightarrow \pi^*$  of aromatic amino acids in BHb. The tryptophan, tyrosine and phenylalanine in the binding cavity of protein have conjugated  $\pi$ -electrons and easily form charge transfer compounds with other electron deficient species or  $\pi$ -electrons system. The interaction of SR24 with BHb included the hydrophobic forces between the aromatic heterocyclic ring and the hydrophobic amino acid residues. Besides peak B, there is another new strong fluorescence peak A. And the excitation wavelength of this peak is 230 nm, which can provide some clues for us to investigate the characteristic of this peak. Comparing with the UV/vis absorbance spectra of BHb (Fig. 1(B), curve c), there is a strong absorption peak around 222 nm and this peak is mainly caused by the transition of  $n \rightarrow \pi^*$  of BHb's characteristic polypeptide backbone structure C=O. According to the corresponding Ref. [45], the conformational changes reflected by the spectral difference at 222 nm in the UV/vis spectra may arise from disturbances of the environment of the polypeptide of the protein. Analyzing from the intensity changes of peak A and peak B, they decreased obviously but to different degree (Table 4): in the absence and presence of SR24, the fluorescence intensity ratios of peak A and peak B are 0.90:1, 0.40:1 and 0.34:1, respectively. We can conclude that the interaction of SR24 with BHb induced the slight unfolding of the polypeptides of protein, which resulted in a conformational change of the protein that increased the exposure of some hydrophobic regions which were previously buried [21]. The above phenomena and the analysis of the fluorescence characteristic of the peaks revealed that the binding of BHb-SR24 induced some micro-environmental and conformational changes in BHb, a complex between BHb and SR24 has formed.

#### 4. Conclusions

This paper presents spectroscopic studies on the interaction of SR24 with BHb by UV/vis absorption, fluorescence, resonance light-scattering spectra (RLS), synchronous fluorescence, and three-dimensional fluorescence spectral techniques. It was shown that the fluorescence of BHb was quenched upon reaction with SR24 as a consequence of complex formation. The quenching belonged to static fluorescence quenching, with non-radiation energy transfer happening within a single molecule. The results revealed the presence of a single class of binding site in the surrounding of Trp and Tyr residues at the interface of BHb; hydrophobic interaction played a major role in stabilizing the complex. The results of synchronous fluorescence spectroscopy and three-dimensional fluorescence spectra indicated that the structure of these Tyr residues environments was altered and the physiological functions of BHb were affected by SR24. The binding study of SR24 with proteins has toxicological importance. This study is expected to provide important insight into the interactions of the physiologically important protein BHb with pesticide. The binding of Sudan dyes to proteins has been exploited in the construction of dye biosensors. Dye biosensor assays can provide measures of the toxic effects of

chemicals on the target organism and of the molecular mechanisms that underlie toxicity.

#### Acknowledgements

We gratefully acknowledge financial support of the Natural Science Foundation of Education Department of Jiangsu Province (Grant No. 07KJA18017), the Jiangsu Fundament of "Qilan Project", and the Scientific Foundation of Yancheng Teachers University.

#### References

- [1] Ertas E, özer H, Alasalvar C. A rapid HPLC method for determination of Sudan dyes and Para red in red chilli pepper. *Food Chemistry* 2007;105:756–60.
- [2] Chailapakul O, Wonsawat W, Siangproh W, Grudpan K, Zhao YF, Zhu ZW. Analysis of Sudan I, Sudan II, Sudan III, and SR24 in food by HPLC with electrochemical detection: comparison of glassy carbon electrode with carbon nanotube-ionic liquid gel modified electrode. *Food Chemistry* 2008;109:876–82.
- [3] Refat NA, Ibrahim ZS, Moustafa GG, Sakamoto KQ, Ishizuka M, Fujita S. The induction of cytochrome P450 1A1 by Sudan dyes. *Journal of Biochemical and Molecular Toxicology* 2008;22:77–84.
- [4] Cornet V, Govaert Y, Moens G, Loco JV, Degroot JM. Development of a fast analytical method for the determination of Sudan dyes in chilli- and curry-containing food stuffs by high performance liquid chromatography-photo-diode array detection. *Journal of Agricultural and Food Chemistry* 2006;54:639–44.
- [5] He LM, Su YJ, Fang BH, Shen XG, Zheng ZL, Liu YH. Determination of Sudan dye residues in eggs by liquid chromatography and gas chromatography-mass spectrometry. *Analytica Chimica Acta* 2007;594:139–46.
- [6] An Y, Jiang LP, Cao J, Geng CY, Zhong LF. Sudan I induces genotoxic effects and oxidative DNA damage in HepG2 cells. *Mutation Research* 2007;627:164–70.
- [7] Mandal R, Kalke R, Li XF. Interaction of oxaliplatin, cisplatin, and carboplatin with haemoglobin and the resulting release of a heme group. *Chemical Research in Toxicology* 2004;17:1391–7.
- [8] Messori L, Gabbiani C, Casini A, Siragusa M, Vincieri FF, Bilia AR. The reaction of artemisinins with haemoglobin: a unified picture. *Bioorganic and Medicinal Chemistry* 2006;14:2972–7.
- [9] Lei C, Wollenberger U, Bistolas N, Guiseppi-Elis A, Scheller FW. Electron transfer of haemoglobin at electrodes modified with colloidal clay nanoparticle. *Analytical and Bioanalytical Chemistry* 2002;372:235–9.
- [10] Scheller FW, Bistolas N, Liu S, Jänchen M, Katterle M, Wollenberger U. Thirty years of haemoglobin electrochemistry. *Advances in Colloid and Interface Science* 2005;116:111–20.
- [11] Bao XY, Zhu ZW, Li NQ. Electrochemical studies of rutin interacting with haemoglobin and determination of haemoglobin. *Talanta* 2001;54:591–6.
- [12] Sil S, Kar M, Chakraborti AS. Studies on the interaction of hematoporphyrin with haemoglobin. *Journal of Photochemistry and Photobiology B: Biology* 1997;41:67–72.
- [13] Liu WJ, Guo X, Guo R. The interaction of haemoglobin with hexadecyltrimethylammonium bromide. *International Journal of Biological Macromolecules* 2005;37:232–8.
- [14] Wang YQ, Zhang HM, Chang GC, Zhou QH, Fei ZH, Liu ZT, et al. Fluorescence spectroscopic investigation of the interaction between benzidine and bovine haemoglobin. *Journal of Molecular Structure* 2008;886:77–84.
- [15] Xi JQ, Guo R. Interactions between flavonoids and haemoglobin in lecithin liposomes. *International Journal of Biological Macromolecules* 2007;40:305–11.
- [16] Yuan JL, Liu H, Kang X, Lv Z, Zou GL. Characteristics of the isomeric flavonoids apigenin and genistein binding to haemoglobin by spectroscopic methods. *Journal of Molecular Structure* 2008;891:333–9.
- [17] Wang YQ, Zhang HM, Zhang GC, Liu SX, Zhou QH, Fei ZH, et al. Studies of the interaction between paraquat and bovine haemoglobin. *International Journal of Biological Macromolecules* 2007;41:243–50.
- [18] Yue YY, Chen XG, Qin J, Yao XJ. A study of the binding of C.I. Direct Yellow 9 to human serum albumin using optical spectroscopy and molecular modeling. *Dyes and Pigments* 2008;79:176–82.
- [19] Shaikh SMT, Seetharamappa J, Ashoka S, Kandagal PB. A study of the interaction between bromopyrogallol red and bovine serum albumin by spectroscopic methods. *Dyes and Pigments* 2007;73:211–6.
- [20] Shaikh SMT, Seetharamappa J, Kandagal PB, Manjunatha DH, Ashoka S. Spectroscopic investigations on the mechanism of interaction of bioactive dye with bovine serum albumin. *Dyes and Pigments* 2007;74:665–71.

- [21] Zhang YZ, Dai J, Zhang XP, Yang X, Liu Y. Studies of the interaction between Sudan I and bovine serum albumin by spectroscopic methods. *Journal of Molecular Structure* 2008;888:152–9.
- [22] Liu YC, Yang ZY, Du J, Yao XJ, Lei RX, Zheng XD, et al. Interaction of curcumin with intravenous immunoglobulin: a fluorescence quenching and Fourier transformation infrared spectroscopy study. *Immunobiology* 2008;213:651–61.
- [23] Hu YJ, Liu Y, Pi ZB, Qu SS. Interaction of cromolyn sodium with human serum albumin: a fluorescence quenching study. *Bioorganic and Medicinal Chemistry* 2005;13:6609–14.
- [24] Alpert B, Jameson DM, Weber G. Tryptophan emission from human haemoglobin and its isolated subunits. *Journal of Photochemistry and Photobiology A: Chemistry* 1980;31:1–4.
- [25] Sulkowska A. Interaction of drugs with bovine and human serum albumin. *Journal of Molecular Structure* 2002;614:227–32.
- [26] Lakowicz JR. *Principles of fluorescence spectroscopy*. New York: Plenum Press; 1999. p. 237.
- [27] Gryczynski Z, Beretta S, Lubkowski J, Razynska A, Gryczynski I, Bucci E. Time-resolved fluorescence of haemoglobin species. *Biophysical Chemistry* 1997;64:81–91.
- [28] Ware WR. Oxygen quenching of fluorescence in solution: an experimental study of the diffusion process. *Journal of Physical Chemistry B* 1962;66:445–8.
- [29] Shang L, Wang YZ, Jiang JG, Dong SJ. pH-dependent protein conformational changes in albumin: gold nanoparticle bioconjugates: a spectroscopic study. *Langmuir* 2007;23:2714–21.
- [30] Klajnert B, Stanislawski L, Bryszewska M, Palecz B. Interactions between PAMAM dendrimers and bovine serum albumin. *Biochimica et Biophysica Acta* 2003;1648:115–26.
- [31] Demchenko AP. The red-edge effects: 30 years of exploration. *Luminescence* 2002;17:19–42.
- [32] Gong AQ, Zhu XS, Hu YY, Yu SH. A fluorescence spectroscopic study of the interaction between epristeride and bovine serum albumin and its analytical application. *Talanta* 2007;73:668–73.
- [33] Wang YQ, Zhang HM, Zhang GC, Tao WH, Tang SH. Binding of brucine to human serum albumin. *Journal of Molecular Structure* 2007;830:b40–5.
- [34] Yan CN, Zhang HX, Liu Y. Fluorescence spectra of the binding reaction between paraquat and bovine serum albumin. *Acta Chimica Sinica* 2005;63:1727–33.
- [35] Ross PD, Subramanian S. Thermodynamics of protein association reaction: forces contribution to stability. *Biochemistry* 1981;20:3096–102.
- [36] Xiao JB, Shi J, Cao H, Wu SD, Ren FL, Xu M. Analysis of binding interaction between puerarin and bovine serum albumin by multi-spectroscopic method. *Journal of Pharmaceutical and Biomedical Analysis* 2007;45:609–15.
- [37] Sklar LA, Hudson BS, Simoni RD. Conjugate polyene fatty acids as fluorescent membrane probes. *Biochemistry* 1977;16:5100–8.
- [38] Haouz A, Mohsni SE, Zentz C, Merola F, Alpert B. Heterogeneous motions within human apohaemoglobin. *European Journal of Biochemistry* 1999;264:250–7.
- [39] Hu YJ, Liu Y, Zhang LX. Study of interaction between colchicines and bovine serum albumin by fluorescence quenching method. *Journal of Molecular Structure* 2005;750:174–8.
- [40] Lloyd JBF. Multicomponent analysis by synchronous luminescence spectrometry. *Nature* 1971;231:64–5.
- [41] Abert WC, Gregory WM, Allan GS. The binding interaction of coomassie blue with protein. *Analytical Biochemistry* 1993;213:407–13.
- [42] Klotz IM. Physicochemical aspects of drug–protein interactions: a general perspective. *Annals of the New York Academy of Science* 1973;226:18–25.
- [43] Li R, Nagai Y, Nagai M. Changes of tyrosine and tryptophan residues in human haemoglobin by oxygen binding: near- and far-UV circular dichroism of isolated chains and recombined haemoglobin. *Journal of Inorganic Biochemistry* 2000;82:93–101.
- [44] Lin GL, Liao YY, Wang XH, Sheng SL, Yin DZ. In situ estimation of the entire color and spectra of age pigment-like materials: application of a front-surface 3D-fluorescence technique. *Experimental Gerontology* 2006;41:328–36.
- [45] Glazer AN, Smith EL. Studies on the ultraviolet difference spectra of proteins and polypeptides. *Journal of Biological Chemistry* 1961;236:2942–7.